

Rogue waves from Optics and Oceanography to Plasma Physics

Ibrahim Elkamash, PhD

Mansoura University, Faculty of Science, Physics Department, Mansoura, Egypt

9th Spring Plasma School at PortSaid (SPSP2024), PortSaid, Egypt.



[nature](#) > [nature reviews physics](#) > [review articles](#) > [article](#)

Review Article | [Published: 23 September 2019](#)

Rogue waves and analogies in optics and oceanography

[John M. Dudley](#) , [Goëry Genty](#), [Arnaud Mussot](#), [Amin Chabchoub](#) & [Frédéric Dias](#)

[Nature Reviews Physics](#) **1**, 675–689 (2019) | [Cite this article](#)



Plasma as a particle (SPM)

- The plasma is a collection of charged particles. So in order to study various physical phenomena inside the plasma, we have to solve the equations of motion:

$$\frac{d\mathbf{r}_i}{dt} = \mathbf{v}_i, \quad (1)$$

$$m_i \frac{d\mathbf{v}_i}{dt} = \mathbf{F}, \quad (2)$$

for each particle.

- Where the position vector \mathbf{r} is given by

$$\mathbf{r} = x\mathbf{x} + y\mathbf{y} + z\mathbf{z}. \quad (3)$$

and the velocity vector \mathbf{v} is given by

$$\mathbf{v} = v_x\mathbf{x} + v_y\mathbf{y} + v_z\mathbf{z}. \quad (4)$$

- \mathbf{F} is the combined influence forced, due to the externally applied forces and the internal forces generated by all the other plasma



Plasma as a gas (Kinetic model)

- So, the three-dimensional plasma kinetic equation becomes:

$$\left[\frac{\partial}{\partial t} + \mathbf{v} \cdot \nabla_{\mathbf{r}} + \frac{\mathbf{F}}{m_s} \cdot \nabla_{\mathbf{v}} \right] f_s(t, \mathbf{r}, \mathbf{v}) = \left(\frac{\partial f_s}{\partial t} \right)_{\text{coll}} \quad (5)$$

- Special cases:

I- If $\left(\frac{\partial f_s}{\partial t} \right)_{\text{coll}} = C(f_s)$: It is called '**Boltzmann**' equation, where $C(f_s)$ is the Coloumb collision operator.

II- If $\left(\frac{\partial f_s}{\partial t} \right)_{\text{coll}} = FP(f_s)$: It is called '**Fokker-Plank**' equation, where $FP(f_s)$ is the FP collision operator.

III- If $\left(\frac{\partial f_s}{\partial t} \right)_{\text{coll}} = 0$: It is called '**Vlasov**' equation. Thus the '**Vlasov**' equation (??) can be simply stated as

$$\frac{df_s}{dt} = 0, \quad (6)$$



Plasma as a fluid (Fluid model)

$$\frac{\partial N_s}{\partial t} + \nabla \cdot [N_s \mathbf{u}_s] = 0,$$

$$m_s N_s \left[\frac{\partial}{\partial t} + \mathbf{u}_s \cdot \nabla \right] \mathbf{u}_s = q_s N_s \left(\mathbf{E} + \mathbf{u}_s \times \mathbf{B} \right) - \nabla P_s + \nabla \cdot \mathbf{\Pi}_s + \mathbf{R}_{ij}$$

$$\frac{\partial \frac{3}{2} P_s}{\partial t} + \nabla \cdot \left(\frac{3}{2} P_s \mathbf{u}_s \right) = P_s \nabla \cdot \mathbf{u}_s + \nabla \cdot \mathbf{q}_s + \mathbf{R}_{ij}$$

$$\text{Gauss' Law} \quad \nabla \cdot \mathbf{E} = \frac{\rho_q}{\epsilon_0},$$

$$\text{Gauss' Law} \quad \nabla \cdot \mathbf{B} = 0,$$

$$\text{Faraday's Law} \quad \nabla \times \mathbf{E} = -\frac{\partial \mathbf{B}}{\partial t}$$

$$\text{Ampère's Law} \quad \nabla \times \mathbf{B} = \mu_0 \mathbf{J} + \mu_0 \epsilon_0 \frac{\partial \mathbf{E}}{\partial t},$$

$$\text{The charge density} \quad \rho_q = \sum q_s N_s,$$

$$\text{The current density} \quad \mathbf{J} = \sum q_s N_s \mathbf{u}_s$$



**Freak
waves**



**Rogue
waves**



**Giant
waves**



**Extreme
waves**



WHAT ARE Rogue WAVES?

- In oceanography:



WHAT ARE Rogue WAVES?

- In oceanography:

i- The amplitude exceeds 3 times the average amplitude, i.e.
Nonlinear Wave



WHAT ARE Rogue WAVES?

- In oceanography:

i- The amplitude exceeds 3 times the average amplitude, i.e.

Nonlinear Wave

ii- Appear from nowhere and disappear without trace, i.e.

Localized in space and Localized in time



WHAT ARE Rogue WAVES?

- In oceanography:

i- The amplitude exceeds 3 times the average amplitude, i.e.
Nonlinear Wave

ii- Appear from nowhere and disappear without trace, i.e.
Localized in space and Localized in time

iii- There is a dip before the hump, i.e.
Focused the energy



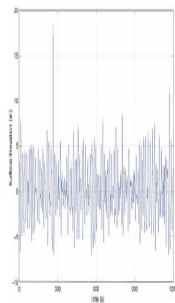
DO Rogue WAVES REALLY EXIST ?



(a) Norwegian tanker Wilstar, Agulhas current (1974)



(b) Oil freighter Esso Languedoc, coast of Durban (1980)



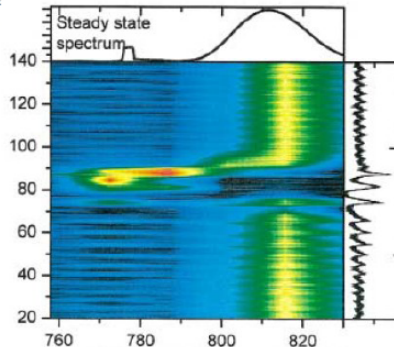
(c) Draupner Platform, the North Sea (New Year's Day 1995)



Experimental Evidence for Soliton Explosions

Steven T. Cundiff,^{1,*} J.M. Soto-Crespo,² and Nail Akhmediev³

We show, experimentally and numerically, that Ti:sapphire mode-locked lasers can operate in a regime in which they intermittently produce exploding solitons. This happens when the laser operates near a critical point. Explosions happen spontaneously, but external perturbations can trigger them. In stable operation, all explosions have the same characteristics of the explosions depend on the intracavity



LETTERS

Optical rogue waves

D. R. Solli¹, C. Ropers^{1,2}, P. Koonath¹ & B. Jalali¹

Recent observations show that the probability of encountering an extremely large rogue wave in the open ocean is much larger than expected from ordinary wave-amplitude statistics^{1–3}. Although considerable effort has been directed towards understanding the physics behind these mysterious and potentially destructive events, the complete picture remains uncertain. Furthermore, rogue waves have not yet been observed in other physical systems. Here, we introduce the concept of optical rogue waves, a counterpart of

Although the physics behind rogue waves is still under investigation, observations indicate that they have unusually steep, solitary or tightly grouped profiles, which appear like “walls of water”^{1,2}. These features imply that rogue waves have relatively broadband frequency content compared with normal waves, and also suggest a possible connection with solitons—solitary waves, first observed by I. S. Russell in the nineteenth century, that propagate without spreading in water because of a balance between dispersion and nonlinearity. As

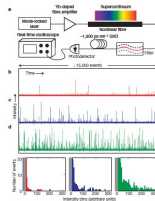


Figure 1 Experimental observation of optical rogue waves. **a**, Schematic of experimental apparatus. **b**, Single-shot time-resolved intensity profiles (10,000 pulses each) and a stack of histograms (bottom of figure left) for the results, as a sign of the average power level (0.01 mW, 0.1 mW, 1.0 mW and 10.0 mW, from top to bottom, respectively). The grey shaded area in each histogram corresponds to the noise floor of the measurement process. In each measurement, the root-mean-square of events $>99.9\%$ for the lowest power are shaded in blue for intensity range, and the average event width is shown in red. At least 10–40 times the average width. These distributions are very different from those encountered in most nonlinear processes.

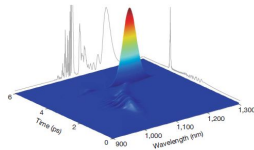


Figure 3 Time-wavelength profile of an optical rogue wave obtained from a short-time Fourier transform. The optical wave has broad bandwidth and has extremely steep slopes in the time domain compared with the typical events. It appears as a ‘wall of light’ analogous to the ‘wall of water’ description of oceanic rogue waves. The rogue wave travels a curved path in time-wavelength space because of the Raman self-frequency shift and group velocity dispersion, separating from non-solitonic fragments and remnants of the seed pulse at shorter wavelengths. The grey traces show the full time structure and spectrum of the rogue wave. The spectrum contains sharp spectral features that are temporally broad and, thus, do not reach large peak power levels and do not appear prominently in the short-time Fourier transform.

[Credit: D.R. Solli, C. Ropers, P. Koonath, B. Jalali, Nature 450, 1054 (2007).]



The Peregrine soliton in nonlinear fibre optics

B. Kibler¹, J. Fatome¹, C. Finot¹, G. Millot¹, F. Dias^{2,3}, G. Genty⁴, N. Akhmediev⁵ and J. M. Dudley^{6*}

The Peregrine soliton is a localized nonlinear structure predicted to exist over 25 years ago, but not so far experimentally observed in any physical system¹. It is of fundamental significance because it is localized in both time and space, and because it defines the limit of a wide class of solutions to the nonlinear Schrödinger equation (NLSE). Here, we use an analytic

Our experiments are designed using the breather formalism of ref. 2. With dimensionless field $\psi(\xi, \tau)$, the self-focusing NLSE is:

$$i \frac{\partial \psi}{\partial \xi} + \frac{1}{2} \frac{\partial^2 \psi}{\partial \tau^2} + |\psi|^2 \psi = 0 \quad (1)$$

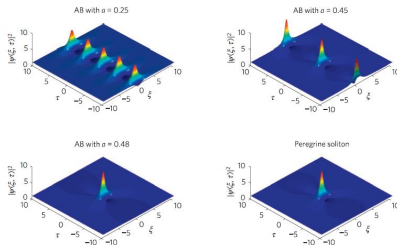


Figure 1 | Plotted Akhmediev breather solutions using equation (2) for modulation parameter $\alpha = 0.25$, $\alpha = 0.45$ and $\alpha = 0.48$, as well as the ideal Peregrine soliton of equation (3), the limiting case of the Akhmediev breather as $\alpha \rightarrow 1/2$. Maximum temporal compression occurs at normalized distance $\xi = 0$. The differences between the Akhmediev breather (AB) with $\alpha = 0.48$ and the Peregrine soliton can be seen with close inspection of the decay of the peak to the wings; they are shown more clearly in Fig. 2.

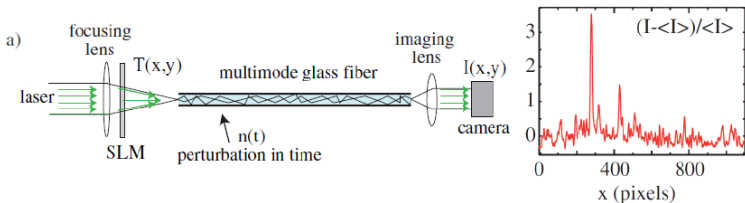
[Credit: B. Kibler, *et al*, Nat. Phys. **6**, 790 (2010)]



Granularity and Inhomogeneity Are the Joint Generators of Optical Rogue Waves

F. T. Arecchi,^{1,2} U. Bortolozzo,³ A. Montina,⁴ and S. Residori³

In the presence of many waves, giant events can occur with a probability higher than expected for random dynamics. By studying linear light propagation in a glass fiber, we show that optical rogue waves originate from two key ingredients: granularity, or a minimal size of the light speckles at the fiber exit, and inhomogeneity, that is, speckles clustering into separate domains with different average intensities. These two features characterize also rogue waves in nonlinear systems; thus, nonlinearity just plays the role of bringing forth the two ingredients of granularity and inhomogeneity.

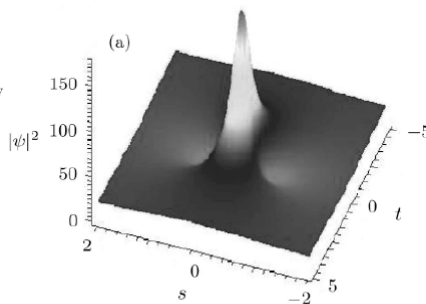


Financial Rogue Waves*

YAN Zhen-Ya (闫振亚)[†]

Key Laboratory of Mathematics Mechanization, Institute of Systems Science
Beijing 100190, China

(Received June 4, 2010)



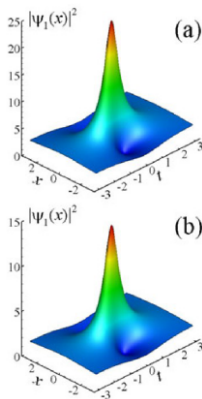
Abstract We analytically give **the financial rogue waves in the nonlinear option pricing model** due to Ivancevic, which is nonlinear wave alternative of the Black–Scholes model. These rogue wave solutions may be **used to describe the possible physical mechanisms for rogue wave phenomenon in financial markets and related fields.**



Vector rogue waves in binary mixtures of Bose-Einstein condensates

Yu.V. Bludov^{1,a}, V.V. Konotop^{2,b}, and N. Akhmediev^{3,c}

Abstract. We study numerically **rogue waves in the two-component Bose-Einstein condensates** which are described by the **coupled set of two Gross-Pitaevskii** equations with variable scattering lengths. We show that rogue wave solutions exist only for certain combinations of the nonlinear coefficients describing two-body interactions. We present the solutions for the combinations of these coefficients that admit the existence of rogue waves.



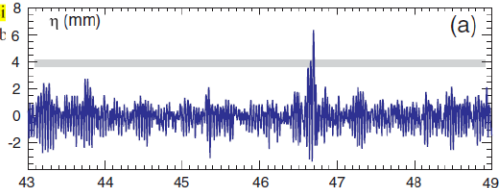
Capillary Rogue Waves

M. Shats,* H. Punzmann, and H. Xia

Research School of Physics and Engineering, The Australian National University, Canberra ACT 0200, Australia

(Received 8 December 2009; published 11 March 2010)

We report the first observation of extreme wave events (rogue waves) in parametrically driven capillary waves. **Rogue waves are observed above a certain threshold in forcing.** Above this threshold, frequency spectra broaden and develop exponential tails. For the first time we present evidence of strong four-wave coupling in nonlinear waves (high tricoherence), which points to modulation instability as the main mechanism in rog **a distinct tail in the** **probability densi** expected from the measured wave b



Rogue Wave Observation in a Water Wave Tank

A. Chabchoub,^{1,*} N. P. Hoffmann,¹ and N. Akhmediev²

¹*Mechanics and Ocean Engineering, Hamburg University of Technology, Eißendorfer Straße 42, 21073 Hamburg, Germany*

²*Optical Sciences Group, Research School of Physics and Engineering, The Australian National University, Canberra ACT 0200, Australia*

(Received 28 February 2011; published 16 May 2011)

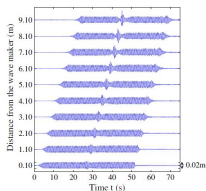
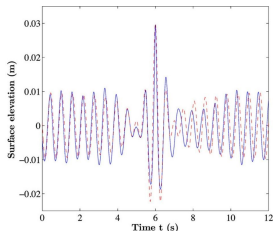


FIG. 3 (color online). Temporal evolution of the water surface height at various distances from the wave maker.



[Credit: A. Chabchoub *et al*, Phys. Rev. Letters 106, 204502 (2011).]



Eur. Phys. J. Special Topics **185**, 57–66 (2010)

© EDP Sciences, Springer-Verlag 2010

DOI: [10.1140/epjst/e2010-01238-7](https://doi.org/10.1140/epjst/e2010-01238-7)

Regular Article

Freak waves in laboratory and space plasmas

Freak waves in plasmas

M.S. Ruderman^a

School of Mathematics and Statistics, University of Sheffield, Hounsfield Road, Hicks Building, Sheffield S3 7RH, UK

Received in final form and accepted 15 June 2010

Published online 23 August 2010



Observation of Peregrine Solitons in a Multicomponent Plasma with Negative Ions

H. Bailung,¹ S. K. Sharma,¹ and Y. Nakamura^{1,2}

¹Plasma Physics Laboratory, Physical Sciences Division, Institute of Advanced Study in Science and Technology, Paschim Boragaon, Guwahati-35, India

²On leave from Yokohama National University, Yokohama, Japan

(Received 29 July 2011; published 16 December 2011)

The experimental observation of Peregrine solitons in a multicomponent plasma with the critical concentration of negative ions is reported. A slowly amplitude modulated perturbation undergoes self-modulation and gives rise to a high amplitude localized pulse. The measured amplitude of the Peregrine soliton is 3 times the nearby carrier wave amplitude, which agrees with the theory. The numerical solution of the nonlinear Schrödinger equation is compared with the experimental results.

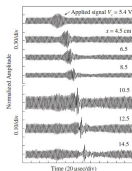


FIG. 2. Observed signals of the electron density perturbation at different probe positions from the separation grid. The top trace is the applied signal with carrier and modulation frequencies 350 and 31 kHz, respectively. Peak to peak amplitude of the applied carrier wave (V_c) is fixed at 5.4 V. Signals observed at 6.5 to 14.5 cm are shown with different amplitude scale (0.10/div) for better resolution.

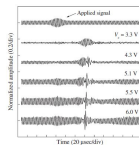


FIG. 3. Signals recorded for different excitation amplitudes of the carrier wave. The probe is fixed at 13.6 cm from the separation grid. Top trace represents the applied signal with carrier and modulation frequencies 350 and 31 kHz, respectively.

[9]. The slight shift in the phase of the carrier part with theory is probably due to the presence of pseudowave in front of the solitons [15]. However, detailed investigation is necessary for confirmation. We analyzed the wave signals

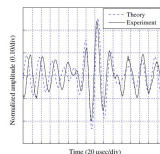


FIG. 4 (color online). Comparison of the time series signal (solid line) observed at 13.6 cm with the theoretical Peregrine soliton (dashed line) obtained by using Eq. (3). The applied carrier and modulation frequencies are 350 and 31 kHz, respectively. $V_c = 5.9$ V. The parameters used for numerical calculations are $\omega = 0.7\omega_p$, ($\omega_0 = 492$ kHz), $k = 0.74k_D$, $k_D = 1/\lambda_D = 200$ cm⁻¹.

[Credit: H. Bailung *et al*, PRL 107, 255005 (2011)]



Generation of acoustic rogue waves in dusty plasmas through three-dimensional particle focusing by distorted waveforms

Ya-Yi Tsai, Jun-Yi Tsai and Lin I*[†]

Rogue waves—rare uncertainly emerging localized events with large amplitudes—have been experimentally observed in many nonlinear wave phenomena, such as water waves^{1,2}, optical waves^{3,4}, second sound in superfluid He II (ref. 5) and ion acoustic waves in plasmas⁶. Past studies have mainly focused on one-dimensional (1D) wave behaviour through modulation instability^{7,8,9,10,11}, and to a lesser extent on higher-dimensional behaviour^{12,13,14,15}. The question whether rogue waves also exist in nonlinear 3D acoustic-type plasma waves, the kinetic origin of their formation and their correlation with surrounding 3D waveforms are unexplored fundamental issues. Here we report the direct experimental observation of dust acoustic rogue waves in dusty plasmas and construct a picture of 3D particle focusing by the surrounding tilted and ruptured wave crests, associated with the higher probability of low-amplitude holes for rogue-wave generation.

Modulation instability (MI) which makes the wave modulation envelope unstable has been well accepted as a mechanism for rogue-wave or envelope soliton generation in systems governed by nonlinear equations, such as the nonlinear Landau–Ginzburg or Schrödinger equations^{16–21,22}. On the other hand, recent studies in nonlinear water, chemical and dust acoustic waves, also demonstrated that MI causes 3D waveform undulation, rupture

(refs 15,16,19,20) are the few examples giving experimental evidence of the ubiquitous behaviour in many other nonlinear media. The advantages of direct video imaging large-area dust density evolution and tracking individual particle motion at the discrete level also make it a good platform to construct an Eulerian–Lagrangian picture as a means of understanding dynamics in nonlinear dusty wave systems^{23,24}. Nevertheless, RWEs have been demonstrated theoretically only in 1D dust acoustic waves²⁵.

The experiment is conducted in a cylindrical radiofrequency (rf) dusty-plasma system, as sketched in Fig. 1a (also see Methods²⁶). Figure 1b shows a typical temporal waveform of n_d , the normalized local dust density, in the disordered state of the self-excited downward propagating DAW. The irregular amplitude modulation evidences MI and causes the broadening of the fundamental and higher harmonic peaks in its power spectrum (Fig. 1c).

Figure 1d shows the histogram of the wave height H measured from 12,000 images. As commonly used for oceanic RWEs, the stretched tail beyond $2H_c$ signifies RWEs, where H_c ($=2$) is the significant wave height, defined as the average of the highest third of all wave heights²⁷. Figure 1e shows the highly localized and randomly distributed RWEs in the xyz space over 120 wave cycles. The averaged wavelength λ and wave period τ_0 are 1 mm and 32 ms, respectively.

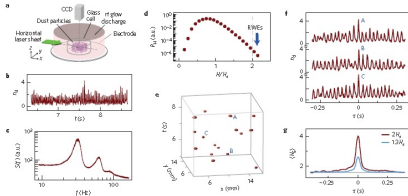


Figure 1 | Experimental system and information evidencing RWEs. a, Sketch of the experimental system. The laser sheet and CCD can also be rotated

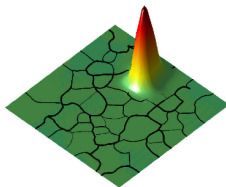


MATHEMATICAL PHYSICS

Mathematicians Tame **Rogue** Waves, Lighting Up Future of LEDs

42 |

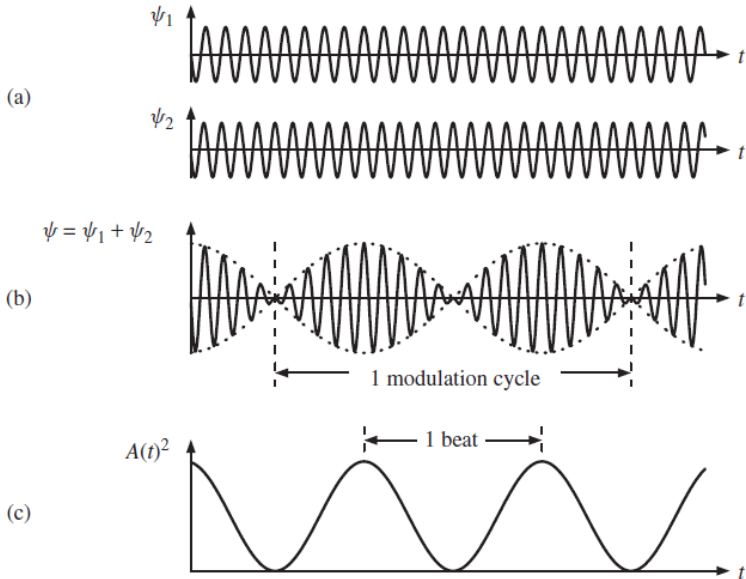
The mathematician Svitlana Mayboroda and collaborators have figured out how to predict the behavior of electrons — a mathematical discovery that could have immediate practical effects.



The black lines are boundaries drawn by the landscape function. They predict the regions where the electronic states remain localized, like the peak shown in this example.



Linear Modulated Wavepackets (AM, FM)



Research Questions

- Questions need to be addressed:



Research Questions

- Questions need to be addressed:

- Is this the case in a nonlinear medium?



Research Questions

- Questions need to be addressed:

- Is this the case in a nonlinear medium?
- Is Rogue wave a critical phenomena?



Research Questions

- Questions need to be addressed:

- Is this the case in a nonlinear medium?
- Is Rogue wave a critical phenomena?
- Is Rogue wave unpredictable phenomena, i.e. Probabilistic phenomena or Deterministic phenomena?



Research Questions

- Questions need to be addressed:

- Is this the case in a nonlinear medium?
- Is Rogue wave a critical phenomena?
- Is Rogue wave unpredictable phenomena, i.e. Probabilistic phenomena or Deterministic phenomena?
- What is the mechanism of formation?



Research Questions

- Questions need to be addressed:

- Is this the case in a nonlinear medium?
- Is Rogue wave a critical phenomena?
- Is Rogue wave unpredictable phenomena, i.e. Probabilistic phenomena or Deterministic phenomena?
- What is the mechanism of formation?
- What are the conditions of the existence?



Plasma System

- System: electrons -ions



Plasma System

- System: electrons -ions
- Boundary Conditions: $L \rightarrow \pm\infty$ (Unbounded).



Plasma System

- System: electrons -ions
- Boundary Conditions: $L \rightarrow \pm\infty$ (Unbounded).
- Initial conditions ($t=0$) (Equilibrium state):

$$n_{e0} = n_{i0} = n_0,$$

$$\phi_0 = 0,$$

$$E_0 = 0,$$

$$T_{e0} = T_{i0} = T_0$$



Plasma System

- System: electrons -ions
- Boundary Conditions: $L \rightarrow \pm\infty$ (Unbounded).
- Initial conditions ($t=0$) (Equilibrium state):

$$n_{e0} = n_{i0} = n_0,$$

$$\phi_0 = 0,$$

$$E_0 = 0,$$

$$T_{e0} = T_{i0} = T_0$$

- Perturbations: Electrical + Thermal (Heating)



Fluid moment equations:

- Density n_α (*continuity*) equation:

$$\frac{\partial n_\alpha}{\partial t} + \nabla \cdot (n_\alpha \mathbf{u}_\alpha) = 0$$

- Mean velocity \mathbf{u}_α equation:

$$\frac{\partial \mathbf{u}_\alpha}{\partial t} + \mathbf{u}_\alpha \cdot \nabla \mathbf{u}_\alpha = -\frac{q_\alpha}{m_\alpha} \nabla \Phi - \frac{1}{m_\alpha n_\alpha} \nabla p_\alpha$$

- Pressure p_α equation: [(*) *Cold* vs. *Warm* fluid model]

$$\frac{\partial p_\alpha}{\partial t} + \mathbf{u}_\alpha \cdot \nabla p_\alpha = -\gamma p_\alpha \nabla \cdot \mathbf{u}_\alpha$$

- The potential Φ obeys *Poisson's eq.*:

$$\nabla^2 \Phi = -4\pi \sum_{\alpha''=\alpha, \{\alpha'\}} q_{\alpha''} n_{\alpha''} = 4\pi e (n_e - Z_i n_i + \dots)$$



Multiscale Perturbation Technique for envelope dynamics

- *1st step.* The idea relies in defining space and time scales, to distinguish the **fast carrier wave** from the **slow envelope** dynamics:

$$X_0 = x, X_1 = \epsilon x, X_2 = \epsilon^2 x, \quad T_0 = x, T_1 = \epsilon x, T_2 = \epsilon^2 x,$$

– + modify the differential space/time operators appropriately:

$$\begin{aligned} \frac{\partial}{\partial x} &\rightarrow \frac{\partial}{\partial X_0} + \epsilon \frac{\partial}{\partial X_1} + \epsilon^2 \frac{\partial}{\partial X_2} + \dots \\ \frac{\partial}{\partial t} &\rightarrow \frac{\partial}{\partial T_0} + \epsilon \frac{\partial}{\partial T_1} + \epsilon^2 \frac{\partial}{\partial T_2} + \dots \end{aligned}$$



Multiscale Perturbation Technique for envelope dynamics

- *2nd step.* Expand the state variables near equilibrium: as

$$\mathbf{S} = \mathbf{S}^{(0)} + \sum_{n=-\infty}^n \epsilon^n \mathbf{S}_n$$

for $\mathbf{S} = (n, u, p, \phi, A)$, i.e.

$$n \approx n_0 + \epsilon n_1 + \epsilon^2 n_2 + \dots$$

$$\mathbf{u} \approx \mathbf{0} + \epsilon \mathbf{u}_1 + \epsilon^2 \mathbf{u}_2 + \dots$$

$$p_\alpha \approx p_0 + \epsilon p_1 + \epsilon^2 p_2 + \dots$$

$$\phi \approx 0 + \epsilon \phi_1 + \epsilon^2 \phi_2 + \dots$$

where $\epsilon \ll 1$ is a *small* real parameter.



Multiscale Perturbation Technique for envelope dynamics

- 2nd step. Expand the state variables near equilibrium: as

$$\mathbf{S} = \mathbf{S}^{(0)} + \sum_{n=-\infty}^n \epsilon^n \mathbf{S}_n$$

for $\mathbf{S} = (n, u, p, \phi, A)$, i.e.

$$n \approx n_0 + \epsilon n_1 + \epsilon^2 n_2 + \dots$$

$$\mathbf{u} \approx \mathbf{0} + \epsilon \mathbf{u}_1 + \epsilon^2 \mathbf{u}_2 + \dots$$

$$p_\alpha \approx p_0 + \epsilon p_1 + \epsilon^2 p_2 + \dots$$

$$\phi \approx 0 + \epsilon \phi_1 + \epsilon^2 \phi_2 + \dots$$

where $\epsilon \ll 1$ is a *small* real parameter.

- 3rd step. Allow for multiple phase-harmonics (**index l**), i.e. multiple phases $2\theta, 3\theta$ etc. to be present at each order n ($= 1, 2, \dots$):

$$\mathbf{S}^{(n)} = \sum_{l=-n}^n \mathbf{S}_n^{(l)}(X_j, T_j) e^{il(kx - \omega t)}$$

denotes the amplitude of the n -th order contribution, as a series of the l -th harmonic amplitude(s)

$\mathbf{S}_n^{(l)} = \mathbf{S}_n^{(l)}(X_j, T_j)$ (*slow*, for $j \geq 1$).

i.e.

$$S \simeq S_0 + \epsilon S_1^{(1)} e^{i(kx - \omega t)} + \epsilon^2 [S_2^{(0)} + S_2^{(1)} e^{i(kx - \omega t)} + S_2^{(2)} e^{i2(kx - \omega t)}] + \dots$$



Governing Equation ($\sim \epsilon^3$)

- Compatibility equation (from $m = 3, l = 1$), in the form of:

$$i \frac{\partial \psi}{\partial \tau} + P \frac{\partial^2 \psi}{\partial \zeta^2} + Q |\psi|^2 \psi = 0.$$

i.e. a *Nonlinear Schrödinger-type Equation (NLSE)* .

- Variables: $\zeta = \epsilon(x - v_g t)$ and $\tau = \epsilon^2 t$;
- *Dispersion coefficient P*:

$$P = \frac{1}{2} \frac{\partial^2 \omega}{\partial k_x^2};$$

- *Nonlinearity coefficient Q*: ...

A (*lengthy!*) function of k , *angle* α and $T_e, T_i, \dots \rightarrow$ (*omitted*).



Nonlinear Frequency Modulation (NFM)

- The total potential disturbance then reads:

$$\phi \simeq \epsilon \hat{\psi} \exp i[kx - (\omega - \epsilon^2 Q |\hat{\psi}|^2) t] + \dots$$

- the net result is

$$\omega \quad \rightarrow \quad \omega - \epsilon^2 Q |\hat{\psi}|^2$$

$$n = n(\psi)$$

which has been verified experimentally!



Nonlinear Frequency Modulation (NFM)

- The total potential disturbance then reads:

$$\phi \simeq \epsilon \hat{\psi} \exp i[kx - (\omega - \epsilon^2 Q |\hat{\psi}|^2) t] + \dots$$

- the net result is

$$\omega \quad \rightarrow \quad \omega - \epsilon^2 Q |\hat{\psi}|^2$$

$$n = n(\psi)$$

which has been verified experimentally!

Fluid: Benjamin-Feir effect,

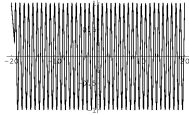
N. Optics: Kerr effect,

Plasma: *nonlinear frequency shift*)



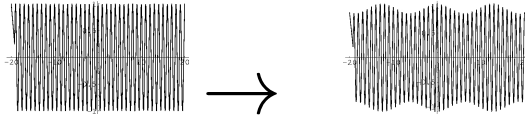
Nonlinear Amplitude Modulation (NAM)

The *amplitude* of a harmonic wave may vary in space and time:



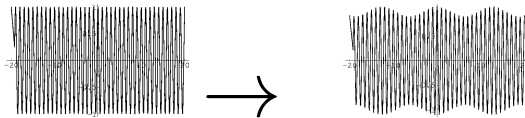
Nonlinear Amplitude Modulation (NAM)

The *amplitude* of a harmonic wave may vary in space and time:



Nonlinear Amplitude Modulation (NAM)

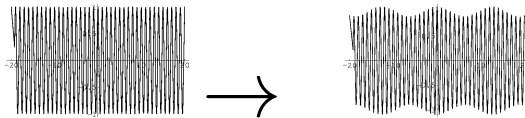
The *amplitude* of a harmonic wave may vary in space and time:



This *nonlinear modulation* (Benjamin-Feir Instability, Kerr Instability, Modulation Instability (MI)):

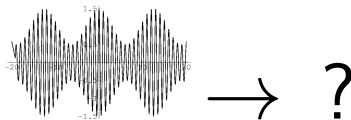
Nonlinear Amplitude Modulation (NAM)

The *amplitude* of a harmonic wave may vary in space and time:



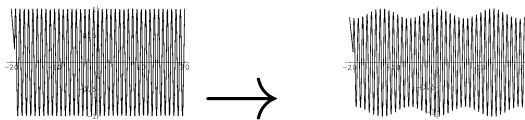
This *nonlinear modulation* (Benjamin-Feir Instability, Kerr Instability, Modulation Instability (MI)):

i-Stable → envelope soliton



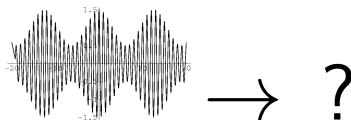
Nonlinear Amplitude Modulation (NAM)

The *amplitude* of a harmonic wave may vary in space and time:

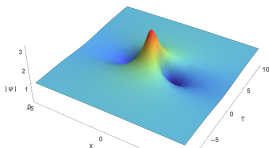


This *nonlinear modulation* (Benjamin-Feir Instability, Kerr Instability, Modulation Instability (MI)):

i- *Stable* → *envelope soliton*



ii- *Unstable* → *Rogue wave*



Rogue wave in Negative ion plasmas

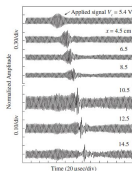
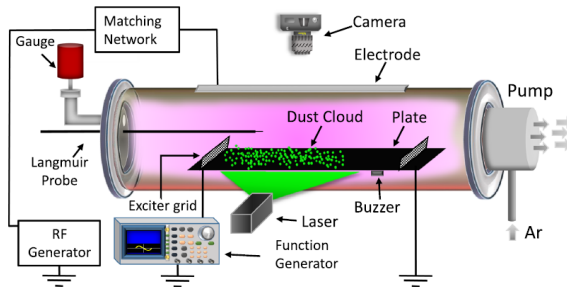


FIG. 2. Observed signals of the electron density perturbation at different probe positions from the separation grid. The top trace is the applied signal with carrier and modulation frequencies 350 and 31 kHz, respectively. Peak to peak amplitude of the applied carrier wave (V_e) is fixed at 5.4 V. Signals observed at 10.5 to 14.5 cm are shown with different amplitude scale (0.10, 0.5) for better resolution.

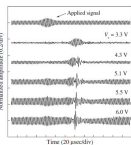


FIG. 3. Signals recorded for different excitation amplitudes of the carrier wave. The probe is fixed at 13.6 cm from the separation grid. Top trace represents the applied signal with carrier and modulation frequencies 350 and 31 kHz, respectively.

[9]. The slight shift in the phase of the carrier part with theory is probably due to the presence of pseudowave in front of the solitons [15]. However, detailed investigation is necessary for confirmation. We analyzed the wave signals

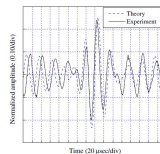


FIG. 4 (color online). Comparison of the time series signal (solid line) observed at 13.6 cm with the theoretical Peregrine soliton (dashed line) obtained by using Eq. (3). The applied carrier and modulation frequencies are 350 and 31 kHz, respectively. $V_e = 5.9$ V. The parameters used for numerical calculations are $\omega = 0.7\omega_{pi}$, ($\omega_{pi} = 492$ kHz), $k = 0.74k_D$, $k_D = 1/\lambda_D = 200$ cm $^{-1}$.

On the occurrence of freak waves in negative ion plasmas

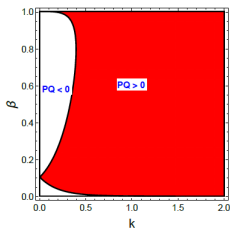
I. S. Elkamash^{1,*}, B. Reville^{2,†} and I. Kourakis^{3,4,‡}

¹ *Physics Department, Faculty of Science,
Mansoura University, 35516 Mansoura, Egypt*

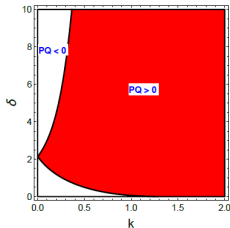
² *Max Planck Institute for Nuclear Physics,
Saupfercheckweg 1, D-69117 Heidelberg, Germany*

³ *Khalifa University, Mathematics Department,
College of Science and Engineering,
P.O. Box 127788, Abu Dhabi, United Arab Emirates*

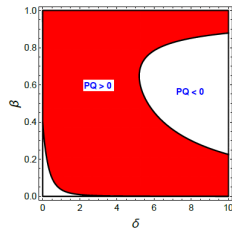
⁴ *Khalifa University, Space and Planetary Science Center,
P.O. Box 127788, Abu Dhabi, United Arab Emirates*



(a)

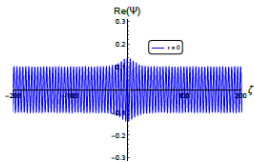


(b)



(c)

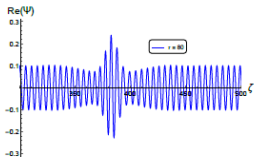




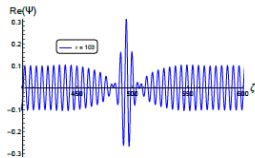
(a)



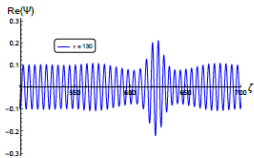
(b)



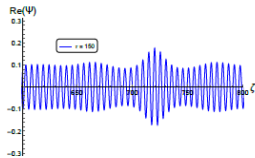
(c)



(d)

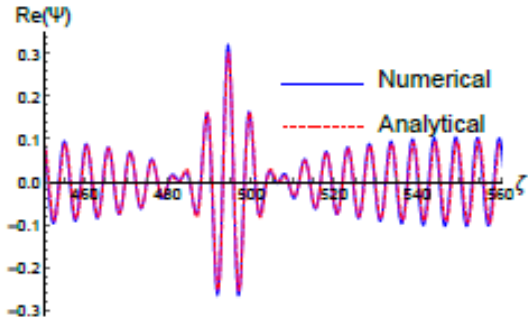


(e)



(f)





Plasma	$\delta (= \frac{Z_n/m_n}{Z_p/m_p})$	$\beta_{cr} (= \frac{n_{0n}Z_n}{n_{0p}Z_p})$
$H^+ - H^- - e^-$	1	0.26
$Ar^+ - F^- - e^-$ (<i>Bailung PRL 2011</i>)	2.1	0.102
$H^+ - O_2^- - e^-$	0.03	0.66
$K^+ - SF_6^- - e^-$	0.267	0.54
$Xe^+ - F^- - e^-$	6.895	0.02
$Ar^+ - O^- - e^-$	1.33	0.2



Conclusions & Summary

- *Amplitude modulation* may be due to various mechanisms, e.g. ponderomotive effects, wave-wave coupling, carrier-wave self-interaction (automodulation); we have here focused on the latter scenario
- *Automodulation* can be modelled via a straightforward multiscale technique
- *Analytical theory predicts:*
 - * **Harmonic generation**
 - * **NL frequency shift**
 - * ***Modulational instability***: Wavepacket propagation is stable for long wavelengths; MI sets in for shorter wavelengths (long wavenumbers)
 - * ***Envelope solitons*** are simply modeled via NLS and related equations
 - * ***Rogue waves*** are random events, may be tedious to detect experimentally;
- Wavepacket propagation is stable for long wavelengths; *Modulational instability* sets in for shorter wavelengths (long wavenumbers);
- Carrier self-interaction (automodulation) is efficiently modeled via a perturbation theory, which also accounts for a) harmonic generation, b) modulational instability, and c) envelope soliton formation;



Thanks for your attention!

